Molecular Cell, Volume *27*

Supplemental Data

A Hierarchical Network of Transcription Factors Governs Androgen Receptor-Dependent Prostate Cancer Growth

Qianben Wang, Wei Li, X. Shirley Liu, Jason S. Carroll, Olli A. Jänne, Erika Krasnickas Keeton, Arul M. Chinnaiyan, Kenneth J. Pienta, and Myles Brown

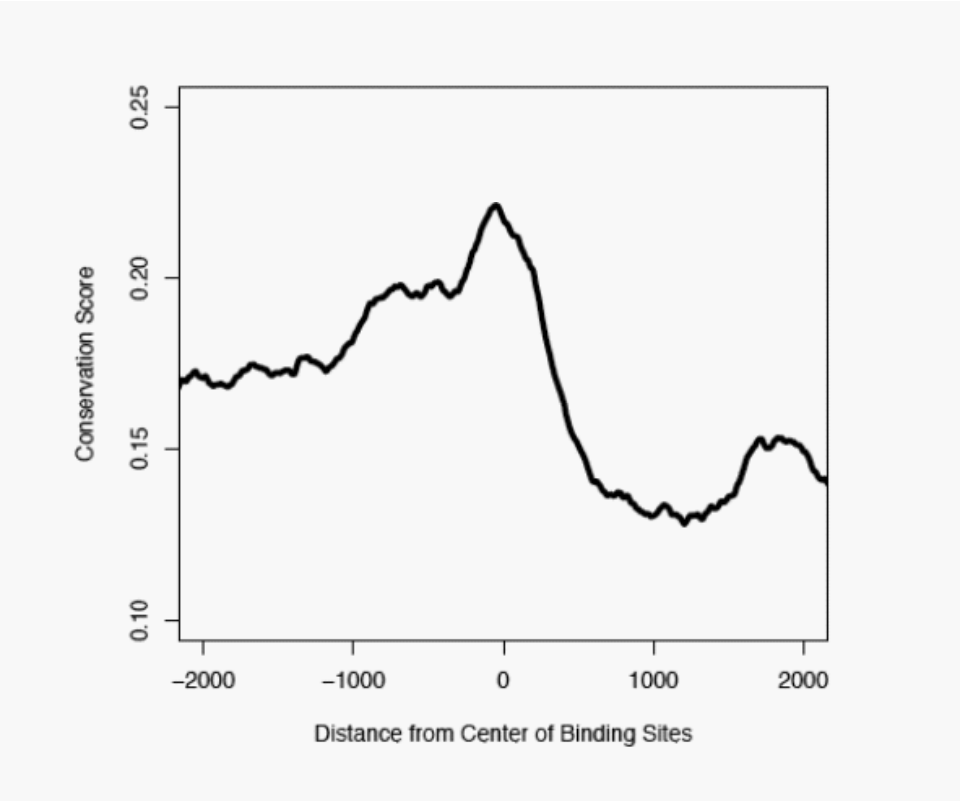

Figure S1: Conservation of AR binding sites based on the alignments of 7 vertebrate genomes (chimp, dog, mouse, rat, chicken, fugu and zebrafish) with human. The center of AR binding regions is designated as coordinate 0, and the distance from the center is shown in nucleotides.

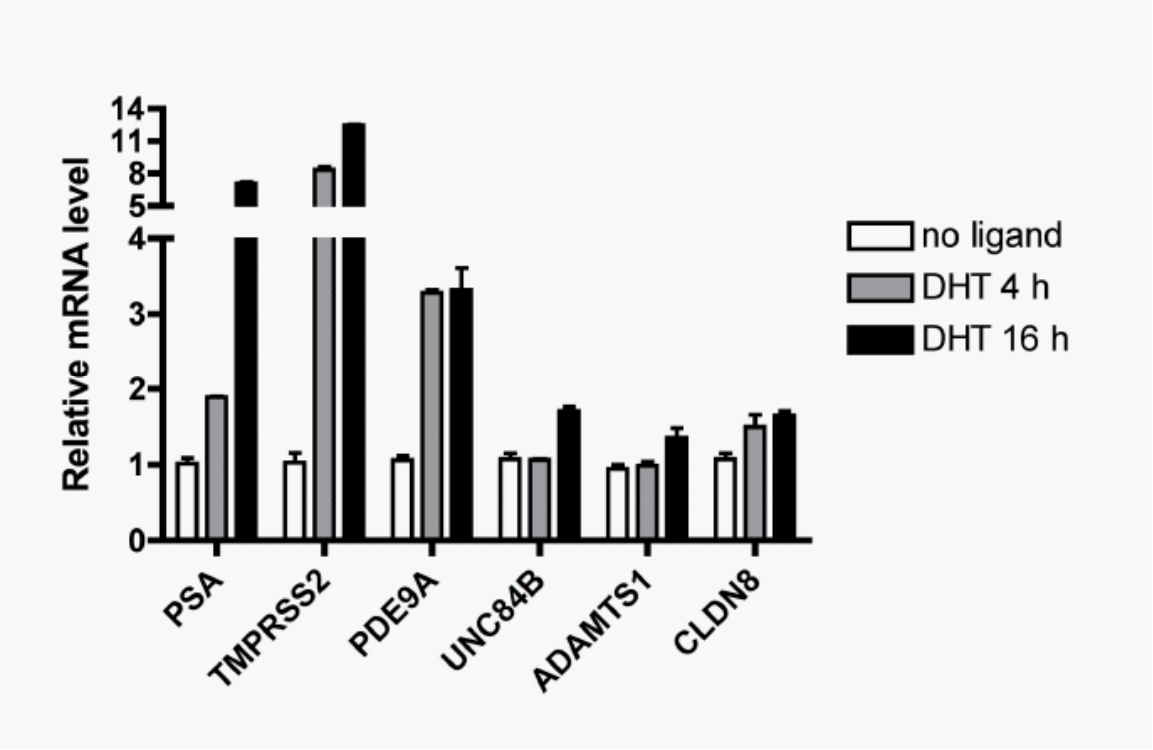

Figure S2: Real-time RT-PCR validation of gene expression changes from the U133 plus 2.0 expression array analyses for six target genes: *PSA*, *TMPRSS2*, *PDE9A*, *UNC84B*, *ADAMTS1*, and *CLDN8* (primers are listed in Table S1). The vehicle control was measured at 4 hr. The data were presented as the mean ± SE of three replicates.

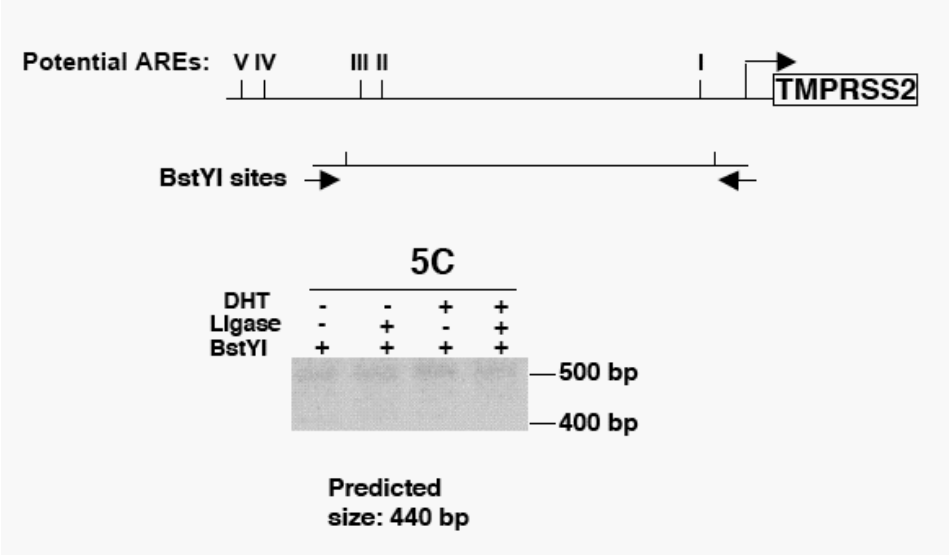

Figure S3: Control for 5C assay. 5C was performed using fixed, BstYI digested chromatin from vehicle- or DHT treated LNCaP cells. Primers (Table S1) flanking the –9 kb AR binding region and –700 bp promoter region were used to PCR amplify DNA after ligation.

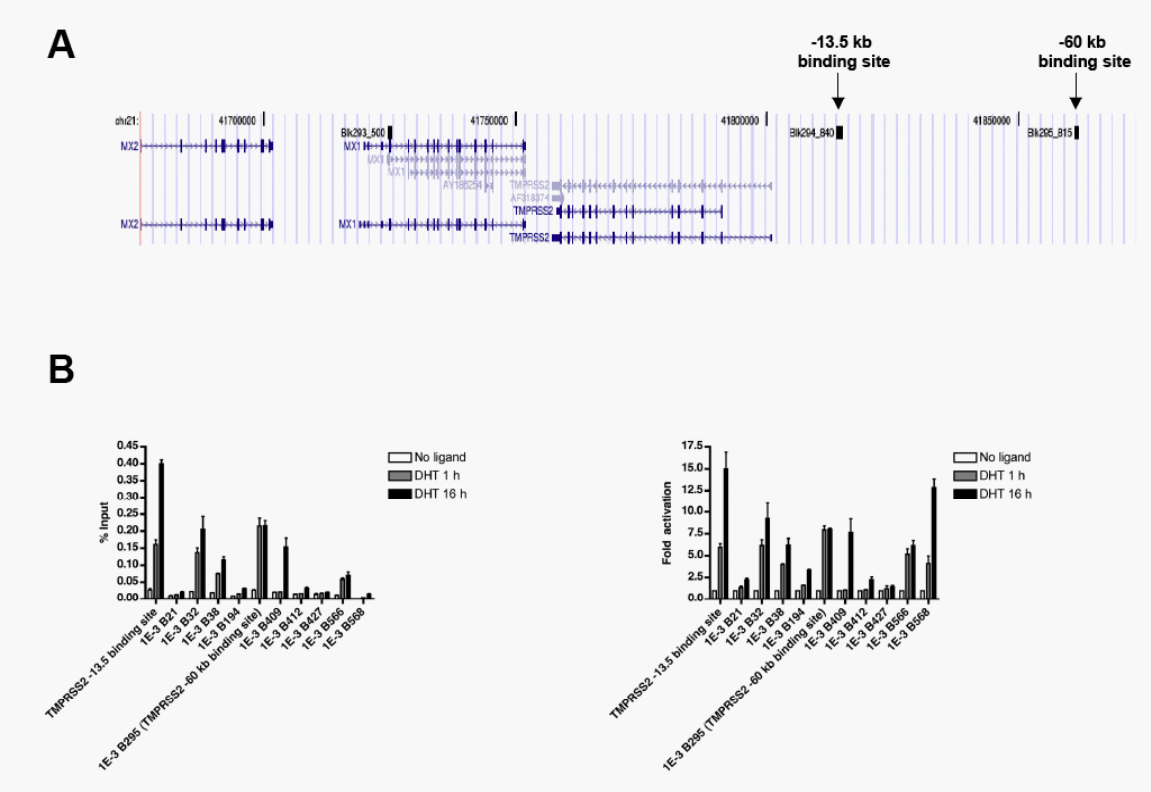

Figure S4: Regular ChIP validation of marginally enriched AR binding regions on chromosomes 21 and 22 (p-value<1E-03). (A) Two AR binding sites relative to the *TMPRSS2* gene. (B) AR ChIP assays were performed on the TMPRSS2 –13.5 kb, –60 kb binding sites and 9 other randomly selected sites. The results were shown as either percentage input (left) or fold enrichment to vehicle control (right).

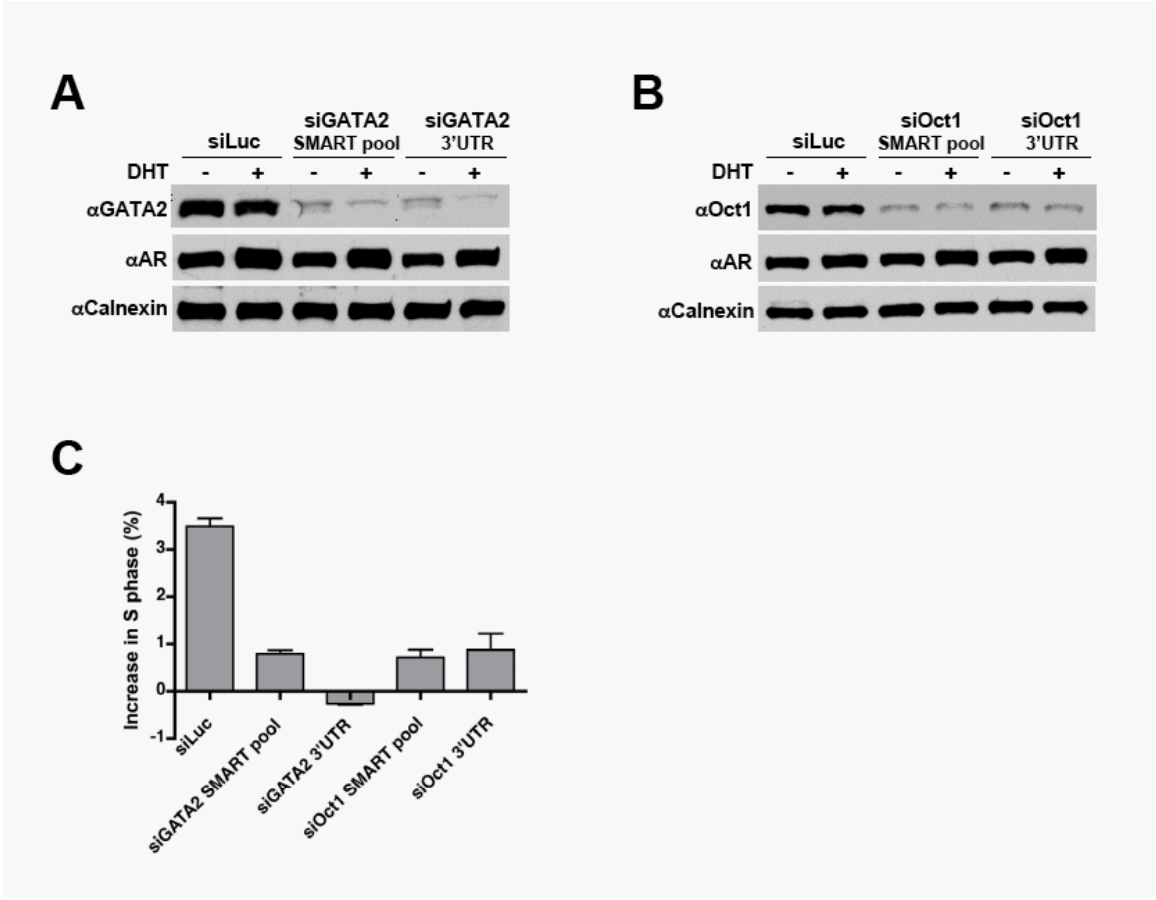

Figure S5: Independent GATA2 and Oct1 siRNAs have same effects on decreasing androgen-stimulated cell cycle progression. GATA2 siRNAs (SMART pool and 3'UTR) and Oct1 siRNAs (SMART pool and 3'UTR) were transfected into LNCaP cells. Western blots (A) and (B) were performed as described in Figure 6A and cell cycle analyses (C) were carried out as described in Figure 7D in the presence or absence of 10 nM DHT. Values represent the mean ± SE of the two independent experiments (C).

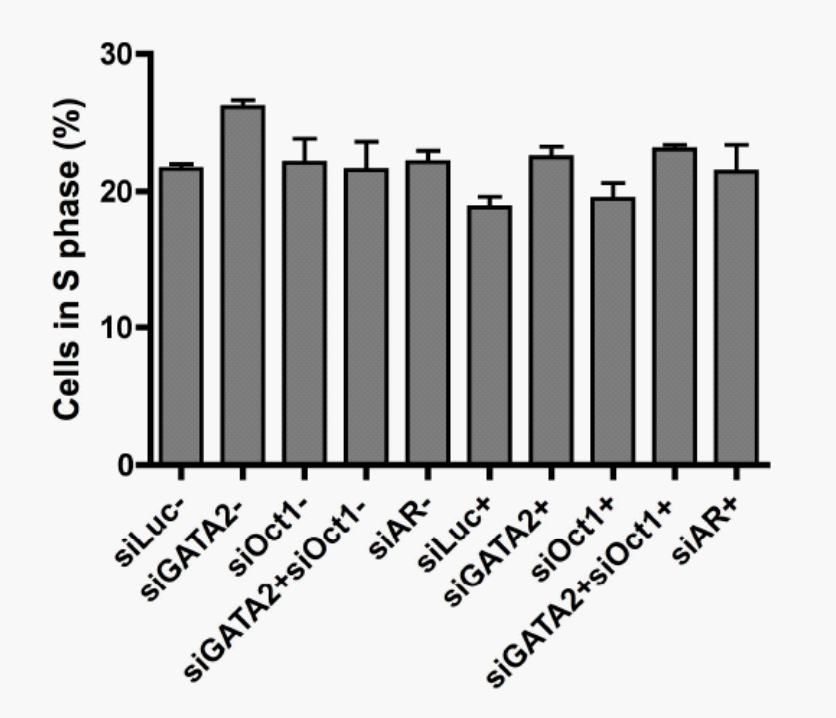

Figure S6: Effects of siRNAs on HeLa cell cycle progression. Forty-eight hours after siRNAs transfection, HeLa cells were treated with vehicle or 10 nM DHT for 24 hr. Cell cycle assays were performed as described in Figure 7D.

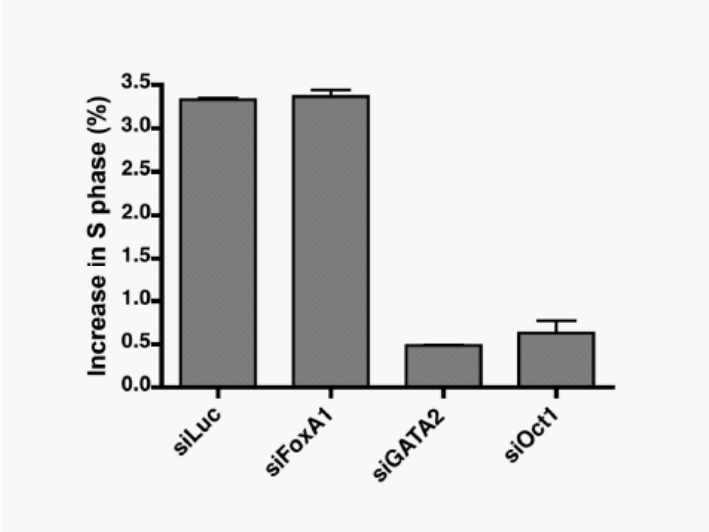

Figure S7. Effects of silencing AR collaborating factors on cell cycle progression. Cell cycle analyses were performed as described in Figure 7D in the presence or absence of 10 nM DHT. The results were presented as the mean ± SE of the two independent experiments.

Table S1: Primer and siRNA sequences

ChIP real-time PCR primers	
Primer name	Sequence (5'-3')
B11+	CTTATCCCCAAGTTGCTGGAAT
B11-	ACGAACAACAGGAATCCATCG
B13+	GAAAGGTCACATTTCTAGCTCGTG
B13-	AAGATGCTATACACATTCCCAAAACA
B19+	CACTACTAAGACATTTCATTTGGTCCA
B19-	AAGAATCTCCAGCAAGCTTTGTG
B20+	CCAAGAACAATCAGTACATGTGGTG
B20-	AAGTGATGGTGATACTATCCTTTGTCA
B21+	GACATGGCGTGACTATAAATAAGGAC
B21-	GCAAACACCTGGTATCAACAGACT
B27+	GAACATGGAGTTCCTGAGAATTTAGG
B27-	TGGTCTAGCAGACAGGCAACA
B30+	TGCTTGACTGAATAAAGATACGGC
B30-	CGGAAGAGTTGTGGGATTCG
B33+	CAGTGGCTTCTCCATCGGAA
B33-	CGTGGGCCAGTGTGTAACAG
B35+	TGGGCCATTGACCTCATAGAG
B35-	AGTCTAATCCTTTGATGCCTGCA
B38+	TGTAGGGAGGGAGCCACACT
B38-	AATGGCCGGGTGTGCC
B39+	TCCAGGCAGAGGTGTGGC
B39-	CGTATGTCTCCCTGCACCACT
B40+	AAGGCAAACAGAGCTGCACA
B40-	TGGTCTGAACGAAGGCGAG
B41+	GCCTCCCCCGTGCAG
B41-	TGCAAGGCACGTCTCAATTC
B44+	CACTCCGTTTCTTAGCCGTGA
B44-	AGGCCTGTGGCTCCCC
B46+	GAGAAAACTCTGACCTGCCGG
B46-	ACTAAGTCATGGTCGAGTCGGAC
B50+	TCACACTTTTGGTATTAGCAAAAGTGA
B50-	GCAAGTGCAAAAGACAAGATGC
B51+	CCTTCCATATCTATCCAGTGCATTTA
B51-	TGGCCTCACACCACTGTTACTT
B52+	TGAAATAATGCTGATTCCTGAGATAAG
B52-	TGCTGGTGCAGGATTTATTCTACT
B58+	CCAAAGGATGCCAAAGTCCA
B58-	TGCCTGCATCCGAGAGATTT
B60+	CTTGTTATCCACCCTTTGCAGTT
B60-	TGACCACGGGAGCCCTAA

ChIP real-time PCR primers (continued)	
Primer name	Sequence (5'-3')
B64+	TCTTCCCTAGCCCGTGATCA
B64-	CAGCCTCCTTTGCAGAGCC
B66+	CCAAAGGATGCCAAAGTCCA
B66-	TGCCTGCATCCGAGAGATTT
B70+	CACCACGGAAGGGAGAAAAG
B70-	TGGGTGATGGGCCGG
B71+	AAGTTACACAGGCGGGCG
B71-	CTGCTCAGGTCTCAGAAAAGGAG
B73+	TTTCCATGTTCTTTTGCCTTTGT
B73-	GGCAGTTGGCATTTACCCG
B77+	AAGCATGTCAACCTGACCTTCA
B77-	AAAGCACCATAAGTGCTGGCA
B85+	AGGAAAGACCCCAGTCCACA
B85-	TCACTGAATTGCCCCTGACTT
B88+	CCAGATACCCGCCTTACAGC
B88-	GCCCCAGGCACAAAACC
B90+	TTTGGGAGCCAGTGATGGA
B90-	AGCCGCCGCCTGAAGT
PSA enhancer+(Wang et al., 2005)	TGGGACAACTTGCAAACCTG
PSA enhancer-(Wang et al., 2005)	CCAGAGTAGGTCTGTTTTCAATCCA
XBP promoter+(Carroll et al., 2005)	TCTGGAAAGCTCTCGGTTTG
XBP promoter-(Carroll et al., 2005)	AATCCCTGGCCAAAGGTACT
pol II control+	GATCTTAGTTGCTTTGCCTCTCTTATC
pol II control-	TTTCTTCTCTTGCCCCTGGA
TMPRSS2 14 kb ARE I+	CTGAGCCCCCACAATTGC
TMPRSS2 14 kb ARE I-	GGTGGGACACACCTCAGCC
TMPRSS2 14 kb ARE II+	TGGATGTTGTCTTTTGTTTTATAATGC
TMPRSS2 14 kb ARE II-	TGCCACTGCACTCCATCCT
TMPRSS2 14 kb ARE III+	CCAGAAGAATACAATGATTAAAAGGCT
TMPRSS2 14 kb ARE III-	TGGAACTGAAGTATTGGAAAACCA
TMPRSS2 14 kb ARE IV+	TCCCAAATCCTGACCCCA
TMPRSS2 14 kb ARE IV-	ACCACACAGCCCCTAGGAGA
TMPRSS2 14 kb ARE V+	TGGTCCTGGATGATAAAAAAAGTTT
TMPRSS2 14 kb ARE V-	GACATACGCCCCACAACAGA
TMPRSS2 –60 kb +	AGGAGGGACCAGAGCCGT
TMPRSS2 –60 kb -	GACACCCAGAAAATACCAGCG
ChIP and 5C assays regular PCR primers	
PSA enhancer+ (Louie et al., 2003)	ATGTTCACATTAGTACACCTTGCC
PSA enhancer- (Louie et al., 2003)	TCTCAGATCCAGGCTTGCTTACTGTC
TMPRSS2 5CEcoRI+	GAGTGTGGTGACTGGCAAAG
TMPRSS2 5CEcoRI/BstYI-	GCCTAGGCTGGCATTTCTT
TMPRSS2 5CBtgI+	CTGGTGAACGCAGGTTGCC

TMPRSS2 5CBtgI-	GCAGAGTCGACATCAGCAAA
TMPRSS2 5CBstYI+	ATGAGCATGAGCTGGAGCCC
B38+	ATCCATCAGCCAACAACTCC
B38-	CACTGTGGGTCTCAGGGTTT
mRNA real-time RT-PCR primers	
PSA mRNA+	TGTGTGCTGGACGCTGGA
PSA mRNA-	CACTGCCCCATGACGTGAT
TMPRSS2 mRNA+	GGACAGTGTGCACCTCAAAGAC
TMPRSS2 mRNA-	TCCCACGAGGAAGGTCCC
PDE9A mRNA+	GATCCCAATGTTTGAAACAGTGAC
PDE9A mRNA-	TCCCAAAGTGGCTGCAGC
UNC84B mRNA+	ATCAGGACGGCGAGCCTAT
UNC84B mRNA-	CCACCTGGTACGTGGCCA
ADAMTS1 mRNA+	GCCAAAGGCATTGGCTACTTC
ADAMTS1 mRNA-	TGGAATCTGGGCTACATGGAG
CLDN8 mRNA+	CGGCTGGAATCATCTTCATCA
CLDN8 mRNA-	TTGGCAACCCAGCTCACAG

Primers for plasmid constructions and mutagenesis	
Primer name	Sequence (5'-3')
B13 enhancer+	AGTGGTACCTTTCTGTTAATGCCATCC
B13 enhancer-	AGGCTCGAGACATCCCAGGAGGGA
B30 enhancer+	GGTGGTACCGCTCTGCTTACACTGGAC
B30 enhancer-	AGGCTCGAGCCTAAGTAATGAGTTTCA
B38 enhancer+	AGTGGTACCTGTGGCCAGTTATGCCGCA
B38 enhancer-	AGGCTCGAGGTCTGGTCTGCAGTCCAGTG
B40 enhancer+	AGTGGTACCAACTCCCTCAAAGATA
B40 enhancer-	ATACTCGAGGTGTGAACCAGGGTGA
B41 enhancer+	AGTGGTACCCTTATGACTAAGCCTGG
B41 enhancer-	ATACTCGAGAGTGGTCTCTCAGCAGAC
B58 enhancer+	AGTGGTACCATACAGCATATAAACAAC
B58 enhancer-	AGGCTCGAGAACAGGAGATGAGAAAGAG
B71 enhancer+	AGTGGTACCCCATGCCAGTGAACAGAG
B71 enhancer-	AGGCTCGAGCGATCTCAATGGAGCAAC
B85 enhancer+	AGTGGTACCCACTCCCGATGACTCCAAAG
B85 enhancer-	AGGCTCGAGCCTTCTTGTTGAACAGTGGGA
B90 enhancer+	AGTGGTACCATTCTGTGAGACCGGGTG
B90 enhancer-	AGGCTCGAGGGTCCAACTCCCAAA
B21 enhancer+	GGTGGTACCTCTATTGTATGTTGATTTC
B21 enhancer-	AGGCTCGAGCACGACCATTTTAGCTC
B21 mutated enhancer+	TTATTAGGGTTGGGATGCACACATTTACCTTTGCCAAATCATT
B21 mutated enhancer-	AATGATTTGGCAAAGGTAAATGTGTGCATCCCAACCCTAATAA
B39 enhancer+	AGTGGTACCATTGCAATAAGAACTTC
B39 enhancer-	AGGCTCGAGGCCTTGTGACACTTCACCC

B39 mutated enhancer+	GTGCAGGGAGACATACGCCCCAATGGCCACCTGGTGAAGTGCA
B39 mutated enhancer-	TGCACTTCACCAGGTGGCCATTGGGGCGTATGTCTCCCTGCAC
FKBP5 enhancer+	AGTGGTACCCTTGGAACACTGATGTG
FKBP5 enhancer-	ATACTCGAGCCAGGTTCCACGCCTG
TMPRSS2 14 kb A+	CGACGCGTAACCATGGAAAGCAGGTGC
TMPRSS2 14 kb A-	CTAGCTAGCAGGGAGGCAGTTGCA
TMPRSS2 14 kb B+	CGACGCGTCTGGGTTCTGGAGCTA
TMPRSS2 14 kb B-	CTAGCTAGCTCTGGTGTGCTGAGGAC
TMPRSS2 14 kb C+	GAACGCGTGATTTGCTTCACCTGGC
TMPRSS2 14 kb C-	CCGGCTAGCGCACTATTTCTACTGC
TMPRSS2 14 kb D+	CGACGCGTTTCTCTGAACATGTG
TMPRSS2 14 kb D-	CCGGCTAGCGGAGATGACTTAATGA
TMPRSS2 14 kb E+	CGACGCGTTTCTCGCTCCTCTCA
TMPRSS2 14 kb E-	CAGGCTAGCTTATGGGCCTGGCGTGA
TMPRSS2 14 kb F+	CTACGCGTGCTCATTGTAGCCTCCG
TMPRSS2 14 kb F-	CAGGCTAGCGTAAGATACACTGGC
TMPRSS2 14 kb G+	CGACGCGTCACCAGTACTTTGATA
TMPRSS2 14 kb G-	CAGGCTAGCCTGATACAGCAGCTGCCA
TMPRSS2 14 kb H+	CGACGCGTTGGCAGCTGCTGTATC
TMPRSS2 14 kb H-	CAGGCTAGCGATCAGGCCTGACCA
TMPRSS2 14 kb I+	CGACGCGTTGGTCAGGCCTGATC
TMPRSS2 14 kb I-	CAGGCTAGCACCTGCTGCCATGCTCA
TMPRSS2 14 kb J+	CAACGCGTTGAGCATGGCAGCAGGTG
TMPRSS2 14 kb J-	CAGGCTAGCATGTGGAGCTCAGCG
TMPRSS2 14 kb K+	CAACGCGTCACGCTGAGCTCCAC
TMPRSS2 14 kb K-	CAGGCTAGCCCATTTAGAAGGCTG
TMPRSS2 14 kb L+	CGACGCGTTCAGCCTTCTAAATGG
TMPRSS2 14 kb L-	CAGGCTAGCTCTCCAGCACATAGG
TMPRSS2 14 kb M+	CGACGCGTCCTATGTGCTGGAGA
TMPRSS2 14 kb M-	CAGGCTAGCACCTGCGTTCACCAG
TMPRSS2 14 kb N+	CGACGCGTGCCGTGTGAGGCAGATAA
TMPRSS2 14 kb N-	TAAGCTAGCCCTCCGCCTCCTGCTTAG
PSA GATA Mt+	AACAAATCTGTTGTAAGAGACAGGACAGTAAGCAAGCCTGGAT
PSA GATA Mt-	ATCCAGGCTTGCTTACTGTCCTGTCTCTTACAACAGATTTGTT
PSA enhancer Oct Mt+	GATATCATCTTGCAAGGATGCCCTTGAAACAACAATCCAGAAA
PSA enhancer Oct Mt-	TTTCTGGATTGTTGTTTCAAGGGCATCCTTGCAAGATGATATC
PSA promoter Oct Mt+	GTCTTAGGGCACACTGGGTCTCTAGGCACGTGAGGCTTTGTAT
PSA promoter Oct Mt-	ATACAAAGCCTCACGTGCCTAGAGACCCAGTGTGCCCTAAGAC
TMPRSS2 GATA Mt+	AATGAAAATGTTGGTCCTGGAAAAAAGTTTTTCACACAGCAAC
TMPRSS2 GATA Mt-	CTTGCTGTGTGAAAAACTTTTTTCCAGGACCAACATTTTCATT
TMPRSS2 Oct Mt+	GGGTACGGCAGGTACTCATATACTTCACCAGGTGGCCATTTGT
TMPRSS2 Oct Mt-	ACAAATGGCCACCTGGTGAAGTATATGAGTACCTGCCGTACCC

siRNA sense sequences	
siRNA name	Sense sequences (5'-3')
siLuc(Wang et al., 2005)	CACUUACGCUGAGUACUUCGA
siFoxA1[2]	GAGAGAAAAAAUCAACAGC
siGATA2(SMART pool sequences from Dharmcon)	(1)UCGAGGAGCUGUCAAAGUG (2)ACUACAAGCUGCACAAUGU (3)GAAGAGCCGGCACCUGUUG (4)GCCCAGGCCUAGCUACUAU
siGATA2 (3'UTR)	ACCCUUAGCAGCCCAGCAU
siOct1 (SMART pool sequences from Dharmcon)	(1)GAAGAAACGCACCAGCAUA (2)GGACAGAUAACUGGGCUUA (3)CAACACAGCAACCGUGAUU (4)ACACCAAAGCGAAUUGAUA
siOct1(3'UTR)	CUGCCAGCCAGGUUAAUAAUC
siAR (SMART pool sequences from Dharmcon)	(1)GGAACUCGAUCGUAUCAUU (2)CAAGGGAGGUUACACCAAA (3)UCAAGGAACUCGAUCGUAU (4)GAAAUGAUUGCACUAUUGA

Table S2. Differentially expressed transcripts on chromosomes 21 and 22.Each gene symbols, the RefSeq and accession numbers, probe set are provided. The fold change and p-value of androgen treatment (4 hr and 16 hr) versus vehicle control is showed.

Symbol	RefSeq	Probe set	Accession	Fold(4 h)	p-value(4 h)	Fold(16 h)	p-value(16 h)
LOC440161 //,	XM_498572 /// XM_498913	243762_at	BF001177	2.88	0.003004	12.13	0.006335
TMPRSS2	NM_005656	226553_at	AI660243	6.54	0.000012	7.4	0.002968
TMPRSS2	NM_005656	211689_s_at	AF270487	6.21	0.00031	7.34	0.003332
TMPRSS2	NM_005656	205102_at	NM_005656	5.29	0.00011	5.83	0.004185
LOC389048	XM_374013	242881_x_at	BG285837	1.4	0.037191	2.11	0.004351
LOC440160	XM_498571	239010_at	AI744280	0.95	0.264726	1.92	0.006999
FLJ30428	XM_086937	226809_at	AW188087	1.12	0.088746	1.84	0.01049
---	XM_497220	228116_at	AW167298	1.08	0.149194	1.71	0.006262
---	XM_498570	242546_at	BE738279	1.07	0.057075	1.68	0.003937
---	XM_498570	231882_at	AL530703	0.95	0.368628	1.58	0.012677
---	---	235445_at	BF965166	1.4	0.022127	1.55	0.021044
PDE9A	NM_001001567 /// NM_001001568 /// NM_001001569 /// NM_001001570 /// NM_001001571	205593_s_at	NM_002606	1.52	0.003156	1.45	0.008983
CLDN8	NM_199328	214598_at	AL049977	1.45	0.001024	1.42	0.004003
ADAMTS1	NM_006988	222486_s_at	AF060152	0.95	0.355998	1.41	0.000787
PRR5	NM_015366 /// NM_017701 /// NM_181333	219168_s_at	NM_017701	0.92	0.421874	1.35	0.007429
ADAMTS1	NM_006988	222162_s_at	AK023795	1.01	0.131073	1.32	0.000757
---	---	218358_at	NM_024324	-0.98	0.31343	1.31	0.025719
C21orf4	NM_006134	225182_at	AL355685	-0.95	0.459743	1.31	0.000933
C21orf106	NM_015151 /// NM_206889 /// NM_206890 /// NM_206891	227199_at	AW027812	1.06	0.108578	1.3	0.000806
UNC84B	NM_015374	212144_at	AL021707	-1.03	0.078084	1.26	0.012726
STCH	NM_006948	202557_at	AI718418	1.06	0.032244	1.23	0.010954
GSTT2	NM_000854	205439_at	NM_000854	0.9	0.505869	1.22	0.045052
C22orf9	NM_001009880 /// NM_015264	212421_at	AB023147	0.93	0.633891	1.22	0.024506
KIAA0153	NM_015140	216251_s_at	BF965437	1.02	0.067989	1.22	0.000728
AP1B1	NM_001127 /// NM_145730	205423_at	NM_001127	1.01	0.148625	1.21	0.001708
KRT18	NM_000224 /// NM_199187	201596_x_at	NM_000224	-0.96	0.567413	1.18	0.042099
C22orf8	NM_017911	219629_at	NM_017911	-0.89	0.555275	1.18	0.010052
C21orf4	NM_006134	219600_s_at	NM_006134	-1.01	0.161066	1.17	0.004024
CGI-96 /// dJ2	--- /// NM_015703	202938_x_at	NM_015703	-0.87	0.981442	1.16	0.016005
SYNJ1	NM_003895 /// NM_203446	212990_at	AB020717	1.76	0.007333	1.16	0.045435
TRPM2	NM_001001188 /// NM_003307	205708_s_at	AI051254	-1.03	0.10008	1.15	0.011701
ARFGAP3	NM_014570	202211_at	BC005122	-0.95	0.678644	1.14	0.022065
LSS	NM_001001438 /// NM_002340	202245_at	AW084510	0.93	0.947085	1.14	0.049552
---	---	232390_at	AL137344	0.95	0.702908	1.14	0.010846
ATXN10	NM_013236	208832_at	AW241832	0.93	0.77761	1.13	0.012443
GAS2L1	NM_006478 /// NM_152236 /// NM_152237	209729_at	BC001782	0.98	0.36676	1.13	0.042922
PP2447	NM_025204	225360_at	AL449244	0.9	0.896766	1.13	0.017823
KIAA0153	NM_015140	1552257_a_at	NM_015140	0.98	0.303255	1.13	0.009713
C22orf9	NM_001009880 /// NM_015264	217118_s_at	AK025608	-0.93	0.902374	1.11	0.014551
TBC1D10A	NM_031937	226613_at	AI742029	0.98	0.258789	1.11	0.031212
PACSIN2	NM_007229	1554691_a_at	BC008037	0.95	0.662284	1.11	0.036146
NHP2L1	NM_001003796 /// NM_005008	201076_at	NM_005008	-1.07	0.021123	1.1	0.012501
C21orf56	NM_032261	223360_at	AL136871	0.92	0.740066	1.1	0.036932
RIPK4	NM_020639	221215_s_at	NM_020639	1.12	0.033472	1.08	0.069483
XBP1	NM_005080	200670_at	NM_005080	-1.13	0.008085	1.07	0.015995
ZNF278	NM_014323 /// NM_032050 /// NM_032051 /// NM_032052	209431_s_at	AF254083	-1.14	0.010689	-1	0.199289
ZNF294	NM_015565	215596_s_at	AL163248	-1.13	0.026142	-1.02	0.160258
MRPL39	NM_017446 /// NM_080794	218558_s_at	NM_017446	-0.95	0.481575	-1.11	0.028839
DSCR5	NM_016430 /// NM_153681 /// NM_153682	221689_s_at	AB035745	-0.99	0.231436	-1.11	0.02614
LOC493856	NM_001008388	226686_at	AI188518	-1.01	0.115249	-1.12	0.004637
LOC493856	NM_001008388	226689_at	AI749451	-0.99	0.239383	-1.13	0.020667
BTG3	NM_006806	205548_s_at	NM_006806	-0.99	0.245993	-1.14	0.009717
FBXO7	NM_012179	1554423_a_at	AF233225	-0.99	0.230398	-1.14	0.034168
FBXO7	NM_012179	201178_at	NM_012179	-1.06	0.021811	-1.16	0.003118
MRPS6	NM_032476	224919_at	AL555227	-1.11	0.035043	-1.21	0.010546
TNRC6B	XM_039385	213254_at	N64803	-1.15	0.026846	-1.24	0.005497
ZCWCC3	NM_015358	213000_at	AP000693	-1.13	0.05195	-1.26	0.014335
ABCG1	NM_004915 /// NM_016818 /// NM_207174 /// NM_207627 /// NM_207628 /// NM_207629 /// NM_207630	204567_s_at	NM_004915	-1.12	0.082917	-1.31	0.031335
---	XM_496541	1569608_x_at	BC016022	-1.07	0.096193	-1.42	0.002574
APOBEC3B	NM_004900	206632_s_at	NM_004900	-0.85	0.612873	-1.56	0.026041
ANKRD20A ///	NM_001012419 /// NM_001012421 /// NM_032250 /// NM_153750 /// XM_496541	1569607_s_at	BC016022	-1.17	0.028292	-1.57	0.001149

Table S3: List of AR binding sites and adjacent androgen-regulated gene locations. Distance to gene transcription start site, gene Refseq number and a brief description, chromosome number, the start and stop site of each AR binding site, block number and length of each AR binding region and -10 X log10 (p-value) are provided.

Distance	RefSeq number and gene description	Chromosome	Start	End	Blk number and length	minus 10Xlog10 (p-value)
-828,277	NM_153750 : C21orf81,hypothetical protein LOC114035	chr21	13446058	13446660	Blk1_602	65.7
-356,978	NM_153750 : C21orf81,hypothetical protein LOC114035	chr21	13917408	13917908	Blk2_500	54.8
324,214	NM_006948 : STCH,stress 70 protein chaperone,	chr21	15001344	15001844	Blk3_500	51.7
779,576	NM_006948 : STCH,stress 70 protein chaperone,	chr21	15456706	15457206	Blk4_500	53.9
1,203,697	NM_006948 : STCH,stress 70 protein chaperone,	chr21	15880827	15881327	Blk5_500	54.1
1,595,497	NM_006948 : STCH,stress 70 protein chaperone,	chr21	16272627	16273127	Blk6_500	52.7
690,352	NM_006806 : BTG3,B-cell translocation gene 3	chr21	18597133	18597633	Blk7_500	50.5
2,252,040	NM_006806 : BTG3,B-cell translocation gene 3	chr21	20158821	20159321	Blk8_500	52.8
3,967,944	NM_006806 : BTG3,B-cell translocation gene 3	chr21	21874727	21875227	Blk9_500	52.2
-2,856,712	NM_017446 : MRPL39,mitochondrial ribosomal protein L39 isoform a	chr21	23044709	23045209	Blk10_500	64.9
-2,082,948	NM_017446 : MRPL39,mitochondrial ribosomal protein L39 isoform a	chr21	23818447	23819001	Blk11_554	95.5
-1,564,814	NM_017446 : MRPL39,mitochondrial ribosomal protein L39 isoform a	chr21	24336608	24337108	Blk12_500	54.5
257,956	NM_017446 : MRPL39,mitochondrial ribosomal protein L39 isoform a	chr21	26159379	26159879	Blk13_500	62
531,312	NM_017446 : MRPL39,mitochondrial ribosomal protein L39 isoform a	chr21	26432734	26433234	Blk14_500	63
276,156	NM_006988 : ADAMTS1,a disintegrin and metalloprotease with	chr21	27415506	27416006	Blk15_500	52.6
309,964	NM_006988 : ADAMTS1,a disintegrin and metalloprotease with	chr21	27449315	27449815	Blk16_500	68.3
480,956	NM_006988 : ADAMTS1,a disintegrin and metalloprotease with	chr21	27620305	27620805	Blk17_500	70.8
-682,656	NM_015565 : ZNF294,zinc finger protein 294	chr21	28604189	28604689	Blk18_500	65.8
-552,908	NM_015565 : ZNF294,zinc finger protein 294	chr21	28733770	28734606	Blk19_836	96.6
-35,112	NM_015565 : ZNF294,zinc finger protein 294	chr21	29251373	29252598	Blk20_1225	151.3
153,176	NM_015565 : ZNF294,zinc finger protein 294	chr21	29440023	29440523	Blk21_500	51.8
157,156	NM_015565 : ZNF294,zinc finger protein 294	chr21	29443961	29444544	Blk22_583	64
265,314	NM_199328 : CLDN8,claudin 8	chr21	30775252	30775752	Blk23_500	63.5
364,732	NM_199328 : CLDN8,claudin 8	chr21	30874580	30875263	Blk24_683	103.6
405,556	NM_199328 : CLDN8,claudin 8	chr21	30915493	30915993	Blk25_500	53.8
1,052,240	NM_199328 : CLDN8,claudin 8	chr21	31562178	31562678	Blk26_500	58.5
-486,392	NM_203446 : SYNJ1,synaptojanin 1 isoform b	chr21	32535463	32535963	Blk27_500	51.1
-175,200	NM_006134 : TMEM50B,transmembrane protein 50B	chr21	33598585	33599260	Blk28_675	76.4
282,476	NM_032476 : MRPS6,mitochondrial ribosomal protein S6	chr21	34084966	34085466	Blk29_500	72.2
995,424	NM_015358 : MORC3,MORC family CW-type zinc finger 3	chr21	35618703	35619203	Blk30_500	68
682,596	NM_015358 : MORC3,MORC family CW-type zinc finger 3	chr21	35931531	35932031	Blk31_500	53.9
192,800	NM_015358 : MORC3,MORC family CW-type zinc finger 3	chr21	36421327	36421827	Blk32_500	51.8
-284,104	NM_153681 : DSCR5,phosphatidylinositol	chr21	37082468	37082968	Blk33_500	59.1
1,007,840	NM_153682 : DSCR5,phosphatidylinositol	chr21	38374844	38375369	Blk34_525	67.6
1,067,004	NM_153682 : DSCR5,phosphatidylinositol	chr21	38434017	38434517	Blk35_500	55.3
1,877,356	NM_153682 : DSCR5,phosphatidylinositol	chr21	39244349	39244894	Blk36_545	79.8
-1,062,740	NM_005656 : TMPRSS2,transmembrane protease, serine 2	chr21	40738958	40739458	Blk37_500	62.5
-462,388	NM_005656 : TMPRSS2,transmembrane protease, serine 2	chr21	41338902	41340223	Blk38_1321	94.6
13,548	NM_005656 : TMPRSS2,transmembrane protease, serine 2	chr21	41815164	41815828	Blk39_664	64.6
-18,424	NM_001001567: PDE9A,phosphodiesterase 9A isoform b	chr21	42965006	42965703	Blk40_697	107.8
-77,824	NM_001001567: PDE9A,phosphodiesterase 9A isoform b	chr21	43024503	43025003	Blk41_500	54.4
372,760	NM_001001188: TRPM2,transient receptor potential cation channel,	chr21	44224742	44225567	Blk42_825	65.9
-396,324	NM_001001188: TRPM2,transient receptor potential cation channel,	chr21	44993987	44994487	Blk43_500	50.7
-752,548	NM_001001188: TRPM2,transient receptor potential cation channel,	chr21	45349880	45351039	Blk44_1159	140.1
-829,136	NM_001001188: TRPM2,transient receptor potential cation channel,	chr21	45426746	45427346	Blk45_600	71.5
-872,476	NM_001001188: TRPM2,transient receptor potential cation channel,	chr21	45470119	45470655	Blk46_536	73.7
-694,120	NM_032261 : C21orf56,hypothetical protein LOC84221	chr21	45734360	45734860	Blk47_500	51.3
-379,184	NM_032261 : C21orf56,hypothetical protein LOC84221	chr21	46049292	46049792	Blk48_500	53.1
76,012	NM_015151 : C21orf106,DIP2-like protein isoform a	chr21	46626352	46628257	Blk49_1905	81.1
-7,973,878	NM_000854 : GSTT2,glutathione S-transferase theta 2	chr22	14653495	14654622	Blk50_1127	99.8
-7,968,730	NM_000854 : GSTT2,glutathione S-transferase theta 2	chr22	14658956	14659456	Blk51_500	56.8
-7,836,959	NM_000854 : GSTT2,glutathione S-transferase theta 2	chr22	14790636	14791319	Blk52_683	85.1
-7,073,373	NM_000854 : GSTT2,glutathione S-transferase theta 2	chr22	15554313	15554813	Blk53_500	58.5
-7,045,991	NM_000854 : GSTT2,glutathione S-transferase theta 2	chr22	15581695	15582195	Blk54_500	59.3
-5,587,958	NM_000854 : GSTT2,glutathione S-transferase theta 2	chr22	17039463	17040494	Blk55_1031	110.7
-5,512,776	NM_000854 : GSTT2,glutathione S-transferase theta 2	chr22	17114462	17115857	Blk56_1395	130.5
-5,453,978	NM_000854 : GSTT2,glutathione S-transferase theta 2	chr22	17173708	17174208	Blk57_500	50.7
-5,434,968	NM_000854 : GSTT2,glutathione S-transferase theta 2	chr22	17192236	17193698	Blk58_1462	338.4
-5,396,068	NM_000854 : GSTT2,glutathione S-transferase theta 2	chr22	17231203	17232533	Blk59_1330	114
-4,856,660	NM_000854 : GSTT2,glutathione S-transferase theta 2	chr22	17771027	17771527	Blk60_500	68.9
-3,907,702	NM_000854 : GSTT2,glutathione S-transferase theta 2	chr22	18719568	18720901	Blk61_1333	110.7
-3,666,566	NM_000854 : GSTT2,glutathione S-transferase theta 2	chr22	18960790	18961950	Blk62_1160	115.2
-3,609,202	NM_000854 : GSTT2,glutathione S-transferase theta 2	chr22	19018484	19018984	Blk63_500	52.3
-2,804,000	NM_000854 : GSTT2,glutathione S-transferase theta 2	chr22	19823222	19824652	Blk64_1430	333.4
-2,761,426	NM_000854 : GSTT2,glutathione S-transferase theta 2	chr22	19866158	19866863	Blk65_705	101.5
-2,683,696	NM_000854 : GSTT2,glutathione S-transferase theta 2	chr22	19943507	19944971	Blk66_1464	344.7
-2,643,440	NM_000854 : GSTT2,glutathione S-transferase theta 2	chr22	19983922	19985069	Blk67_1147	105.6
-2,637,100	NM_000854 : GSTT2,glutathione S-transferase theta 2	chr22	19990586	19991086	Blk68_500	54.6
-2,529,376	NM_000854 : GSTT2,glutathione S-transferase theta 2	chr22	20098309	20098809	Blk69_500	51.6
-2,241,148	NM_000854 : GSTT2,glutathione S-transferase theta 2	chr22	20386495	20387082	Blk70_587	77.7
-1,400,962	NM_000854 : GSTT2,glutathione S-transferase theta 2	chr22	21226647	21227301	Blk71_654	89.2
-492,764	NM_000854 : GSTT2,glutathione S-transferase theta 2	chr22	22134923	22135423	Blk72_500	61.5
-434,552	NM_000854 : GSTT2,glutathione S-transferase theta 2	chr22	23081177	23081677	Blk73_500	50.5
-1,619,062	NM_000854 : GSTT2,glutathione S-transferase theta 2	chr22	24265688	24266188	Blk74_500	61
104,074	NM_005080 : XBP1,X-box binding protein 1	chr22	27624921	27625458	Blk75_537	61.9
28,844	NM_001127 : AP1B1,adaptor-related protein complex 1 beta 1 subunit	chr22	28137717	28138217	Blk76_500	56.3
129,024	NM_001127 : AP1B1,adaptor-related protein complex 1 beta 1 subunit	chr22	28237771	28238525	Blk77_754	98.2
534,224	NM_014323 : ZNF278,zinc finger protein 278 long C isoform	chr22	30600779	30601279	Blk78_500	50.5
-1,458,496	NM_015374 : UNC84B,unc-84 homolog B	chr22	36017703	36018203	Blk79_500	51.6
-574,140	NM_015374 : UNC84B,unc-84 homolog B	chr22	36902057	36902557	Blk80_500	58
31,792	NM_015374 : UNC84B,unc-84 homolog B	chr22	37507991	37508491	Blk81_500	54.9
-1,058,860	NM_004900 : APOBEC3B,apolipoprotein B mRNA editing enzyme, catalytic	chr22	38761515	38762015	Blk82_500	52.2
-1,345,044	NM_004900 : APOBEC3B,apolipoprotein B mRNA editing enzyme, catalytic	chr22	39047698	39048198	Blk83_500	54.8
-723,852	NM_005008 : NHP2L1,NHP2 non-histone chromosome protein 2-like 1	chr22	39678954	39679454	Blk84_500	50.2
-21,944	NM_015264 : C22orf9,hypothetical protein LOC23313 isoform a	chr22	43906460	43907421	Blk85_961	102.8
-92,544	NM_017911 : C22orf8,hypothetical protein LOC55007	chr22	44118644	44119144	Blk86_500	60.2
-146,192	NM_013236 : ATXN10,ataxin 10	chr22	44534165	44534665	Blk87_500	57
-1,398,484	NM_013236 : ATXN10,ataxin 10	chr22	45785608	45787806	Blk88_2198	206
-1,540,192	NM_013236 : ATXN10,ataxin 10	chr22	45927204	45929627	Blk89_2423	86.3
-1,620,736	NM_013236 : ATXN10,ataxin 10	chr22	46008479	46009437	Blk90_958	117.2

Table S4. List of typical AREs and non-typical AREs in 90 AR binding regions. Four types non-typical ARE: 1) ARE half-site, AGAACA (score cutoff is 7.0, corresponding to its exact match); 2) ARE head to head, AGAACA[0-8n]TGTTCT; 3) ARE tail to tail, TGTTCT[0-8n]AGAACA; 4) ARE direct repeat, AGAACA[0-8n]AGAACA (type 2 to 4, score cutoff 8.5, allowing the 0-8 bases variable gap between two AR half-sites) and typical ARE (AGAACAnnnTGTTCT) (score cutoff 8.5, allowing only 3 bases gap between two AR half-sites) are listed for 90 AR binding regions.

	Typical ARE	AR half-site	Head to Head	Tail to Tail	Direct Repeat
Blk1		7.3 TGTTCT	8.9 TGAACT 6 TGTTCT	8.7 TGTTCC 3 ACAACA	8.9 TGAACT 6 TGTTCT
Blk2					
Blk3					
Blk4					8.9 TGGTCT 0 TGATCT
Blk5			8.6 AGAAAA 5 TTTTCT		8.7 AGGACA 2 AGAAAA
Blk6					8.9 AGAGCA 4 AGCACA
Blk7		7.3 TGTTCT		8.9 TGTCCT 2 AGAACT	8.6 TTTTCT 4 TATTCT
Blk8					
Blk9					8.6 AGAATA 4 AGAAAA
Blk10			8.7 AAAACA 6 TGGTCT	8.6 TGTTTT 3 AAAACA	8.6 TGTTTT 2 TGTTTT
Blk11		7.3 TGTTCT			8.7 TTCTCT 8 TGTTCT
Blk12				8.7 TGTTCA 4 AGAAAA	
Blk13		7.3 TGTTCT	8.6 AAAACA 1 TTTTCT	11.6 TGTTCT 2 ACAACA	8.6 ACAACA 2 AGAAAA
Blk14					
Blk15				8.7 TGTTCA 5 ATAACA	8.9 AGAGCA 4 AGAACG
Blk16		7.3 AGAACA	8.7 ACAACA 0 TGTACT		11.6 AAAACA 8 AGAACA
Blk17		7.3 TGTTCT		14.6 TGTTCT 3 AGAACA	8.7 ATTTCT 3 TGTTCT
Blk18		7.3 TGTTCT	8.7 AAAACA 7 TGTTCA		8.7 TTTGCT 0 TGTTCT
Blk19	8.9 AGTACA 3 TGTGCT				8.6 TGTTTT 0 TGTTTT
Blk20		7.3 AGAACA	8.7 AGAACT 4 TGTTGT		8.6 AAAATA 8 AGAACA
Blk21	8.9 AGTACA 3 TGTTCC				
Blk22		7.3 TGTTCT	8.7 AGAAGA 0 GGTTCT		8.6 TTTTGT 7 TGTTCT
Blk23		7.3 TGTTCT		8.7 TGTTCT 4 ACAACC	8.7 TGTTCT 8 TGTTAC
Blk24	8.9 AGAACA 3 TGATCA	7.3 AGAACA			8.9 AGAACA 3 TGATCA
Blk25					
Blk26					8.7 TATTCT 0 TGTTCC
Blk27					
Blk28					8.7 TTTTCT 3 GGTTCT
Blk29		7.3 TGTTCT	8.9 AGGACT 1 TGTTCT		8.6 AGAAGA 5 AGAATA
Blk30		7.3 TGTTCT	11.6 AGAATA 7 TGTTCT	8.7 TTTTCT 0 AGATCA	11.6 TATTCT 3 TGTTCT
Blk31		7.3 TGTTCT		8.7 TGTTCT 7 CCAACA	8.9 TGTTCT 3 TGATCC
Blk32					
Blk33		7.3 AGAACA			8.7 AGAACA 1 TAAACA
Blk34		7.3 AGAACA		8.9 TGTACT 5 AGCACA	8.9 GGAACC 0 AGAACA
Blk35		7.3 AGAACA		8.9 TGACCT 5 AGAACA	8.7 TGATCT 1 TGTTGT
Blk36		7.3 AGAACA		8.7 ATTTCT 7 AGAACA	8.9 AGAACA 5 GGAGCA
Blk37		7.3 TGTTCT	8.7 GCAACA 7 TGTTCT		8.7 AGAACA 6 GAAACA
Blk38	11.7 AGAACA 3 TGTGCT	7.3 AGAACA	8.6 AGAAGA 8 TGTTTT	8.9 TGTACA 2 AGAACA	8.9 TGTACA 2 AGAACA
Blk39			8.7 ACAACA 8 TGTCCT		
Blk40		7.3 TGTTCT			8.7 TGATTT 4 TGTTCT
Blk41	14.6 AGAACA 3 TGTTCT	7.3 TGTTCT			8.9 TGGGCT 5 TGTTCT
Blk42					8.6 TTTTCT 8 TCTTCT
Blk43					
Blk44		7.3 TGTTCT	8.7 AGAACA 8 TGATGT	8.9 TGTTCC 5 AGATCA	8.7 TGTGTT 7 TGTTCT
Blk45			8.7 AGACCA 8 TGTTGT		
Blk46		7.3 AGAACA	8.6 AGAACA 2 TCTTTT		8.9 AGTTCT 2 TGTTCA
Blk47					
Blk48					
Blk49					
Blk50		7.3 TGTTCT	8.6 AGAAAA 2 TCTTCT	8.7 TGCTCT 8 AGAAAA	8.7 TGTTCT 2 TGTGAT
Blk51		7.3 AGAACA		8.7 TGCTAT 6 AGAACA	8.7 AGATCA 8 AAAACA
Blk52	8.7 AGAAGA 3 AGTTCT				
Blk53					
Blk54					8.7 TGTTAT 1 TGTGCT
Blk55			8.7 AGAAAA 5 TGTTCC		8.7 TGTGCT 8 TTTTCT
Blk56		7.3 AGAACA	8.9 AGAACA 2 TGGCCT	11.7 TGGTCT 5 AGAACA	8.7 TGTTAT 7 TGGTCT
Blk57		7.3 AGAACA	8.6 AGAATA 0 TTTTCT		8.7 AGAACA 3 AGAAAC
Blk58		7.3 TGTTCT	8.7 ATAACA 4 AGTTCT	8.7 TTTTCT 5 AGAACC	8.9 TGGCCT 5 TGTTCT
Blk59			8.7 AGAAAA 5 TGTTCC		8.7 TGTGCT 8 TTTTCT
Blk60					
Blk61			8.7 GGAACA 5 TTTTCT		8.7 AGAAAA 8 AGCACA
Blk62			8.7 AGAAAA 5 TGTTCC		8.7 TGTGCT 8 TTTTCT
Blk63		7.3 AGAACA	8.7 AGAACA 7 TGATTT		8.6 TGTTTT 5 TGTTTT
Blk64		7.3 AGAACA	8.9 GGAACA 8 TGTTCA	8.9 CGTACT 7 AGAACA	8.9 GGTACA 1 AGAACA
Blk65			8.7 GGAACA 5 TTTTCT		8.7 AGAAAA 8 AGCACA
Blk66		7.3 TGTTCT	8.7 ATAACA 4 AGTTCT	8.7 TTTTCT 5 AGAACC	8.9 TGGCCT 5 TGTTCT
Blk67			8.7 AGAAAA 5 TGTTCC		8.7 TGTGCT 8 TTTTCT
Blk68					
Blk69				8.7 TGTTTT 8 AGATCA	
Blk70		7.3 TGTTCT			8.9 GGTACT 6 TGTTCT
Blk71			8.7 AGACCA 1 TGTTTT	8.9 TGTTCA 7 GGAACA	8.6 AAAACA 1 AAAACA
Blk72					
Blk73		7.3 TGTTCT	8.7 AAAACA 1 TGATCT	8.7 TGTTCT 8 AGACTA	11.6 TGTTCT 8 TGTTTT
Blk74					
Blk75		7.3 TGTTCT			8.9 TGTTCT 5 TGACCT
Blk76		7.3 AGAACA	8.7 AGAACA 4 TGTTTC	8.6 TCTTTT 8 AGAACA	8.9 TGTTCC 5 TGCTCT
Blk77		7.3 TGTTCT	8.9 GGCACA 6 TGTTCT	8.6 TGTTCT 0 AAAAGA	8.7 AGAACA 4 AGATGA
Blk78		7.3 AGAACA	8.7 AGAAAA 4 TGCTCT	8.9 TGCTCT 6 AGACCA	8.7 TGAACA 5 AGAAAA
Blk79	8.9 AGAACA 3 TGTGCC	7.3 AGAACA			8.7 AAAACT 4 AGAACA
Blk80					
Blk81					
Blk82	8.9 AGAACA 3 TGCACT	7.3 AGAACA			8.9 AGAACA 8 AGAGCG
Blk83		7.3 TGTTCT		8.9 TGACCT 1 AGAACA	8.9 GGTTCC 3 TGTTCT
Blk84					
Blk85		7.3 TGTTCT		8.7 TGTTCT 7 TTAACA	8.6 AGAAAA 1 ACAACA
Blk86	11.7 AGGACA 3 TGTTCT	7.3 TGTTCT			8.6 TTTTCT 3 TGTTGT
Blk87					8.9 AGACCA 3 AGAGCA
Blk88		7.3 AGAACA			8.7 TGTTCC 1 TGTTGT
Blk89					
Blk90		7.3 AGAACA			

Supplemental Experimental Procedures

ChIP-on-chip data analysis

To ensure there is only one probe measurement within any 1 kb window, the short-range (< 1 kb) repetitive probe measurements in tiling arrays were filtered out as previously described (Li et al., 2005). Quantile normalization (Bolstad et al., 2003) was used to make the distribution of probe intensities the same across all arrays. A generalized Mann-Whitney U-test, considering probe by probe variability, was then used for the ChIP-enriched region detection. Briefly, (PM-MM) values for each probe are transformed into ranks across the ChIP and control experiments to remove probe variability, followed by regular Mann-Whitney U-test on the ranks over each 1 kb sliding window. The p-value was derived from the null hypothesis that the treatment set median is no larger than that of the control set. Two treatments (100 nM DHT 1 hr and 16 hr) and two controls (vehicle and genomic input) experiments were performed (3 biological replicates each). The ChIP-enriched regions were identified for each treatment against each control (1 hr-vehicle, 1 hr-input, 16 hr-vehicle, 16 hr-input,) using a stringent p-value cutoff 1E-05. The resulting four sets of regions were merged together to form the 90 nonredundant AR binding regions.

Sequence analysis

The repeat-masked genomic DNA of every AR binding regions was retrieved from http://genome.ucsc.edu. We applied the MDscan motif finding algorithm (Liu et al., 2002) on the 90 AR binding regions ranked by p-value score, but could not find any sequence pattern resembling the typical palindrome ARE consensus (AGAACAnnnTGTTCT) (Verrijdt et al., 2003).

We used the positional weight matrix to scan the entire AR binding regions for the inexact matches to the typical and non-typical AREs. The positional weight matrix for AR half-site is derived directly from the ARE consensus as AGAACA. We determined how well a given sequence segment of width w matched a motif (positional weight matrix) as the maximum score from the following scoring formula applied on the sequence segment itself and its reverse complement:

$$S = \sum_{i=1}^{w} \sum_{j \in \{A,C,G,T\}} \delta_{ij} \ln\left(\frac{p_{ij} + p_s}{b_j}\right)$$

Where p_{ij} is the frequency of nucleotide j at position i in the motif, p_s is a pseudocount of 0.04, b_j is the background probability of nucleotide j calculated from the intergenic regions of the human genome. δ_{ij} =1 if nucleotide j is present at position i; $\delta_{ij} = 0$ otherwise. The score for typical ARE is computed by summing the 12 positional weights corresponding to the ARE consensus, allowing 3-nt spacing between two half-sites. Despite choosing a relatively loose score cutoff of 8.5 (corresponding to up to 2 bases difference from the ARE consensus), we identified only 9 ARE occurrences in the 90 AR binding regions. For non-typical ARE, we allowed a variable gap of 0-8 bases between the two AR half-sites and allowed the AR half-sites to be in all possible orientations (Verrijdt et al., 2003) including head to head AGAACA[0-8n]TGTTCT, tail to tail TGTTCT[0-8n]AGAACA, and direct repeat AGAACA[0-8n]AGAACA. The score cutoff (8.5) is the same for the typical ARE. We also considered the exact matches to the AR half-site (score cutoff 7.0) as another kind of non-typical AREs.

In order to identify the cooperative binding partner of AR, we mapped all the mammalian transcription factor motifs in the TRANSFAC database (Matys et al., 2003)

to the nonrepetitive sequences of human chromosomes 21 and 22. We chose score cutoffs from 4.0 to 14.0 at 0.5 intervals for each TRANSFAC motif, and required the minimum number of motif hits in the 90 AR binding regions to be greater than 20. For each motif at each score cutoff, we calculated the fold-enrichment of this motif co-occurring with AR half-site in the 90 AR binding regions compared with that in the human chromosomes 21 and 22 genomic background. When we ranked all the motifs by the maximum fold-change, Forkhead, GATA, Oct motifs that are associated with AR half-site came on top of the list. The p-value associated with each fold-change was derived from the one-tailed binomial test.

We expanded all 90 AR binding sites equally in both directions to 4 kb long. The phastCons (Siepel et al., 2005) conservation scores for alignments of 7 vertebrate genomes (chimp, dog, mouse, rat, chicken, fugu and zebrafish) with human were downloaded from http://genome.ucsc.edu. The conservation score of each nucleotide in the expanded binding region is further defined as the average phastCons scores of a 500-mer window centered at the nucleotide.

ChIP and re-ChIP

Antibodies used were as follows: anti-RNA pol II (8WG16) from Covance (Berkeley, CA), anti-AR (N20), anti-TRAP220 (M255), anti-HNF3α (H120), anti-GATA2 (H116), anti-Oct1 (C21), and rabbit IgG (sc2027) from Santa Cruz Biotechnology (Santa Cruz, CA). For re-ChIP assays, ChIPs were first performed with anti-AR antibodies (N20). The immunoprecipitated complexes were washed, eluted with 10 mM dithiothreitol at 37 °C for 30 min and diluted 50 times with ChIP dilution buffer. The second

immunoprecipitation were then performed with IgG or indicated antibodies. The PCR primers for ChIP and re-ChIP are listed in Table S1.

Reporter gene assays

Twenty-four hours after transfection, cells were treated with 100 nM DHT or vehicle for another 24 hr and then harvested. Transfection efficiency was normalized by co-transfection of pRL promoter renilla luciferase vector (Promega). Firefly and renilla luciferase activity were measured using the Dual-Glo lucifearse assay kit (Promega).

Co-immunoprecipitation and Western blotting

Hormone-depleted LNCaP cells were treated with or without 100 nM DHT for 24 hr. The cells were lysed in 1 ml of ice-cold buffer A. The lysate was rotated for 1 hr at 4°C and precleared by 25 μl of packed protein A-Sepharose. 10 μg IgG or specific antibodies against AR collaborating factors were then added and immunoprecipitation was performed overnight. After immunoprecipitation, 25 μl of packed protein A-Sepharose were added for 1 hr and the beads were washed with lysis buffer A twice. The precipitated protein complexes were fractionated by 8% SDS-PAGE and Western blotting were performed with an anti-AR (441) antibody. The same membranes were then reprobed with antibodies against AR collaborating factors. Antibodies used were anti-AR (441), anti-HNF3α (H120), anti-GATA2 (H116), anti-GATA2 (CG296), anti-Oct1 (C21), and anti-Oct1 (12F11) from Santa Cruz Biotechnology, anti-FoxA1 (ab5095) from Abcam (Cambridge, CA).

Supplemental References

Bolstad, B. M., Irizarry, R. A., Astrand, M., and Speed, T. P. (2003). A comparison of normalization methods for high density oligonucleotide array data based on variance and bias. Bioinformatics *19*, 185-193.

Carroll, J. S., Liu, X. S., Brodsky, A. S., Li, W., Meyer, C. A., Szary, A. J., Eeckhoute, J., Shao, W., Hestermann, E. V., Geistlinger, T. R., *et al.* (2005). Chromosome-wide mapping of estrogen receptor binding reveals long-range regulation requiring the forkhead protein FoxA1. Cell *122*, 33-43.

Li, W., Meyer, C. A., and Liu, X. S. (2005). A hidden Markov model for analyzing ChIP-chip experiments on genome tiling arrays and its application to p53 binding sequences. Bioinformatics *21 Suppl 1*, i274-i282.

Liu, X. S., Brutlag, D. L., and Liu, J. S. (2002). An algorithm for finding protein-DNA binding sites with applications to chromatin-immunoprecipitation microarray experiments. Nat Biotechnol *20*, 835-839.

Louie, M. C., Yang, H. Q., Ma, A. H., Xu, W., Zou, J. X., Kung, H. J., and Chen, H. W. (2003). Androgen-induced recruitment of RNA polymerase II to a nuclear receptor-p160 coactivator complex. Proc Natl Acad Sci U S A *100*, 2226-2230.

Matys, V., Fricke, E., Geffers, R., Gossling, E., Haubrock, M., Hehl, R., Hornischer, K., Karas, D., Kel, A. E., Kel-Margoulis, O. V., *et al.* (2003). TRANSFAC: transcriptional regulation, from patterns to profiles. Nucleic Acids Res *31*, 374-378.

Siepel, A., Bejerano, G., Pedersen, J. S., Hinrichs, A. S., Hou, M., Rosenbloom, K., Clawson, H., Spieth, J., Hillier, L. W., Richards, S., *et al.* (2005). Evolutionarily conserved elements in vertebrate, insect, worm, and yeast genomes. Genome Res *15*, 1034-1050.

Verrijdt, G., Haelens, A., and Claessens, F. (2003). Selective DNA recognition by the androgen receptor as a mechanism for hormone-specific regulation of gene expression. Mol Genet Metab *78*, 175-185.

Wang, Q., Carroll, J. S., and Brown, M. (2005). Spatial and temporal recruitment of androgen receptor and its coactivators involves chromosomal looping and polymerase tracking. Mol Cell *19*, 631-642.